An Elastic Cache Infrastructure through Multi-level Load-balancing

Carlos Lübbe and Bernhard Mitschang
IPVS, University of Stuttgart, Universitätsstraße 38, 70569 Stuttgart, Germany

Keywords: Load-balancing, Spatial Cache, Spatial Data Processing, Peer-to-Peer System.

Abstract: An increasing demand for geographic data compels data providers to handle an enormous amount of range queries at their data tier. In answer to this, frequently used data can be cached in a distributed main memory store in which the load is balanced among multiple cache nodes. To make appropriate load-balancing decisions, several key-indicators such as expected and actual workload as well as data skew can be used. In this work, we make use of an abstract mathematical model to consolidate these indicators. Moreover, we propose a multi-level load-balancing algorithm which considers the different indicators in separate stages. Our evaluation shows that our multi-level approach significantly improves the resource utilization in comparison to existing technology.

1 INTRODUCTION

Geographic data is becoming increasingly important, since the rapid proliferation of Internet-ready mobile devices have made location based services (LBS) accessible to a large crowd of users. As LBS typically operate on data referring the user's current vicinity, data providers need to be able to cope with a massive amount of requests for data of specific geographic regions. A lot of these requests can be cached in a distributed main memory store which provides efficient access to most frequently used data. Key players make use of similar concepts to cope with massive load, e.g. Facebook uses Memcached to cache frequently used data in main memory and many others make highly requested data on dedicated edge servers available. In such a distributed system, it is essential to balance incoming load among participating cache nodes to provide high throughput during the entire execution process. For that matter, specific challenges have to be considered.

First of all, spatial data is not spread uniformly across the world but rather relates to the density of geographic features or the degree of development of represented areas. As obviously more cache memory is needed to cover regions with high data density than sparsely occupied areas, it is essential to consider *data skew* to adequately allocate cache memory during load-balancing. Furthermore, the workload is not equally scattered throughout the data space. In fact, large areas are likely to be not requested at all, as approximately 70% of the world is covered by water being typically of little interest by the majority of people. Thus, it is crucial to consider the *expected workload* and reserve resources for those areas which are most likely to be requested. Finally, effective load balancing must also react to *dynamic load peaks* when the actual workload deviates from anticipated patterns.

Existing load-balancing mechanisms are limited to one of the three above-mentioned indicators. For instance, (Aberer et al., 2005), focuses on data skew only, (Scholl et al., 2009), addresses only expected workload and many other approaches, such as (Lübbe et al., 2012; Wang et al., 2005), solely focus on dynamic load-peaks. Fully relying on a single indicator can lead to inadequate resource allocation during load-balancing.

To substantiate our argument, we use an example of a maritime region comprising little islands and a huge offshore portion. In this area, the data is distributed nonuniformly with higher concentration in insular regions. An oil spill, ship wreckage or any other critical event will suddenly raise disproportionately high interest in the area around the event's location. In consequence, a purely dynamic approach clusters a huge amount of memory to cache data in the sea area around the accident, although at that location only marginal data exists. This overcompensation can lead to poor resource utilization which compromises the overall performance of the system, as the resources would have been needed elsewhere, e.g., to

Lübbe C. and Mitschang B..
An Elastic Cache Infrastructure through Multi-level Load-balancing.
DOI: 10.5220/0004486001830190
In *Proceedings of the 2nd International Conference on Data Technologies and Applications* (DATA-2013), pages 183-190
ISBN: 978-989-8565-67-9

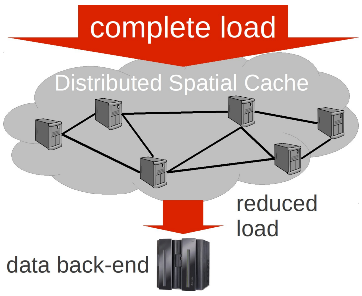

Figure 1: Overview.

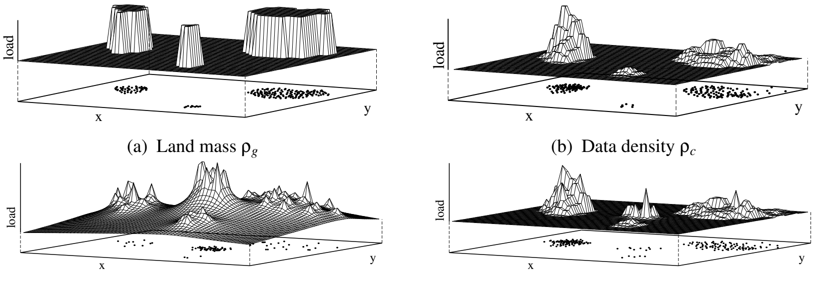

(a) Land mass ρ_g (b) Data density ρ_c (c) Actual workload ρ_d (d) Holistic distribution ρ_h

Figure 2: Examples for distribution functions (Lübbe et al., 2013).

cache data of insular regions.

The different load-balancing indicators data skew, expected workload and dynamic load peaks can all be consolidated into a comprehensive mathematical model (Lübbe et al., 2013). In this work, we implement a distributed and elastic main memory cache supporting multi-level load-balancing which considers the different indicators of the abstract model in separate stages. The first stage prepares the cache network for expected workload while the second adapts to unexpected load peaks. We systematically evaluate the approach in the above-mentioned realistic scenario. Our evaluation shows that our implementation significantly improves the resource utilization in comparison to a conventional algorithm.

2 FOUNDATIONS

As this paper builds upon the ideas of previous work (Lübbe et al., 2011; Lübbe et al., 2012; Lübbe et al., 2013), this section outlines their major contributions. First, we describe the general architecture of the distributed main memory cache. Then, we present a strategy to to control the overall cache content of participating cache nodes. Finally, we summarize our abstract load-balancing model.

Overview. (Lübbe et al., 2011) introduced data structures and algorithms to store spatial data on a single node. The work bases on a general data model comprising objects which contain an obligatory attribute delineating the spatial extend of the object and arbitrary additional non-spatial attributes. Thus, a single node can use the cached objects of previous queries to process a given range query. Combining multiple of these cache nodes to a distributed spatial main memory cache, allows scalable access to frequently used data. Figure 1 depicts the general architecture of such a system. In the distributed infrastructure, cache nodes process requests cooperatively using the cached data of previous queries and may fetch missing data from the data back-end which stores the complete data set. Due to the considerable high spatial and temporal overlap between succeeding queries, most requests can be served by the distributed spatial cache which leads to a reduction of back-end accesses. To achieve a high cache hit-rate during execution, it is essential to control the cache content of participating nodes as elaborated in the following.

Cache Content Control. To control the overall cache content of the distributed spatial cache, (Lübbe et al., 2012) introduced a dedicated replacement strategy, denoted as *focused caching*. In this strategy, we assign each cache node a point in space, denoted as its *cache focus*. Once the capacity of a node has been reached, the node replaces the data with the highest Euclidean distance to its cache focus in order to free up space for new data. As a single node will thus rather keep data near its cache focus, the overall cache content can be controlled by moving the cache foci of participating nodes into certain regions. Increasing the density of cache foci in a geographic area also enlarges the amount of memory allocated for that region and thus raises the cache hit-rate for queries which request data of that particular region. This observation forms the basis of this paper's approach which positions the cache foci according to dedicated distribution functions characterized in the following.

Abstract Distribution Model. In (Lübbe et al., 2013), we introduced an abstract mathematical model to describe load distributions as probability density functions. Formally, such a distribution function can be defined as a two-dimensional function $\rho : \mathbb{R}^2 \rightarrow \mathbb{R}$ which maps geographic coordinates to an abstract measure representing load. To balance load, we can use such distribution functions to distribute the resources, i.e. the cache foci, in the same way.

Load distribution functions can be classified into *anticipated*, *dynamic* and *holistic distributions*. *Anticipated distributions* express statistical analysis of previous workloads, heuristic assumptions about the expected workloads or prior knowledge on data skew.

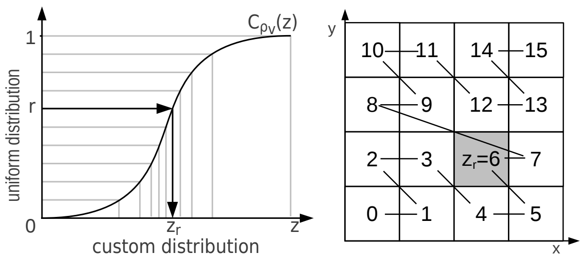

(a) Cumulative distribution (b) Z-Curve

Figure 3: Generate custom distributions of cache foci.

These indicators play an important role in finding an adequate resource allocation, as they enable to prepare for expected situations before the actual load strikes the system. For instance, assuming that users mainly request onshore data we can define ρ_g which returns 1 in onshore regions 0 otherwise, as depicted in Figure 2(a). A resource allocation according to this function distributes the cache foci uniformly within land parts and cuts out the sea areas. This coarse model can be refined by function ρ_c which returns the number of objects per area. As shown in the bottom part of Figure 2(b) this clusters the cache foci in regions with high density and thus increases the cache memory for data-intensive areas. *Dynamic distributions* measure the actual workload at a certain point in space. Our example ρ_d uses the positions of the cache foci to situate the node's current workload (queries per second) in space. Due to unforeseen load peaks, the actual workload may deviate from anticipated patterns, as visualized by the high peak in the middle of Figure 2(c). With regard to the negligible amount of data present in this area, we can observe a clear oversupply of cache memory. For this reason, it can be beneficial to fuse multiple aspects into a single *holistic distribution*. Our example ρ_h incorporates ρ_c and ρ_d in equal shares. Thus, we obtain an allocation which prioritizes regions where both workload and data density is high, as observable in Figure 2(d).

3 IMPLEMENTATION

This section describes the concrete implementation of the abstract load-balancing model. For that we integrated the example distribution functions of the abstract model into our system (see Section 3.1). Based on link structures among the nodes of the cache network, we propose a flexible reorganisation scheme supporting multi-level load-balancing (see Section 3.2). Finally, we implement an algorithm which uses the distribution functions of the abstract model to realize multi-level load-balancing (see Section 3.3).

3.1 Integrating Distributions

The distribution functions of Figure 2 form an example of a concrete load-balancing model which is likely to be needed by a service provider of an LBS. Other application domains may require different models, however. For this reason, our system supports arbitrary load-balancing models by the inclusion of custom distribution functions. From these custom distribution functions, we derive resource allocations (i.e. distributions of cache foci) which are tailored towards the service provider's specific needs. In the following, we present a method to calculate the positions of cache foci using custom distributions. During our example, we use a two-dimensional Gaussian distribution, denoted as ρ_v, as representative for an arbitrary custom distribution.

With probabilistic methods, a standard uniform random number generator can be extended to do this task. Best practices for the one-dimensional case can be found in (Grinstead et al., 2006). However, additional efforts are required for our two-dimensional functions. For this reason, we applied a z-ordering (Morton, 1966) to discretize a given distribution function ρ_v and to map the two-dimensional coordinates to one dimension. For each of the z-numbers, we precomputed the corresponding function values of ρ_v and composed the cumulative distribution function $C_{\rho_v}(z) = \sum_{i=0}^{i=z} \rho_v(x_{z_i}, y_{z_i})$, where x_{z_i}, y_{z_i} represent the two-dimensional coordinates of the z-number z_i. The inverse of C_{ρ_v} can be used to obtain random z-numbers according to the original distribution function ρ_v. As depicted in Figure 3(a), the z-numbers which correspond to the uniform samples of the ordinate have the same frequencies as defined by our Gaussian distribution function ρ_v. Thus, for a given uniform random number r with $0 \leq r < 1$, we used $C_{\rho_v}^{-1}$ to retrieve the corresponding the z-number z_r. To obtain the final result, we generate a uniformly distributed random point within the corresponding cell of z_r (see Figure 3(b)). These points closely match the distribution function ρ_v (minus a negligible discretization error). With this method, we can produce scattered point sets of any distribution function, such as our examples of Figure 2. Note, that any space-filling curve could have been used for this task. We used a z-ordering because it is straightforward to implement and yet very efficient to compute. For our evaluation scenario (see Section 4) we achieved sufficient results in terms of transformation accuracy with a 5th order z-curve which comprises 32 cells in each dimension, i.e., 1024 cells in total.

3.2 Network Structure

In our system model, we assume the cache nodes to be connected via a communication protocol such as the Internet Protocol (IP), i.e., nodes can send or receive messages using distinct network addresses. On top of this communication structure, we assume a large number of nodes that can unexpectedly join or leave our network of cache nodes. Each node keeps the network addresses of a respectably small subset of nodes, thus limiting the impact of unexpected node join or departure to local parts of the cache network. When two nodes mutually know their network addresses, we say they are connected via a link. Similar to common peer-to-peer models such as (Stoica et al., 2001), every node in the cache network can be reached via multiple-hop routing over the links. We continue with a detailed description of distributed request processing, describe how to maintain the cache network and finally propose a mechanism to reorganize the network structure during load-balancing.

Distributed Query Processing. To enable efficient processing of range queries, the geographic relation of the data being cached by the nodes has to be reflected in the link structure of the cache network. A Delaunay triangulation of the cache foci constitutes such a link structure which preserves the topological relationship. Figure 4 depicts a Delaunay triangulation where triangle vertices (black dots) represent the cache foci and the triangle edges (bold lines) represent links between the corresponding nodes. The Delaunay property is met when no vertex exists which is inside the circumcircle of any other triangle (a formal definition can be found in e.g. (de Berg et al., 2000)). In a Delaunay-based link topology, it is possible to apply greedy routing, i.e., a node forwards a given query to the neighbor that has the closest cache focus to the requested query region until no closer neighbor is found. The node at which greedy routing terminates processes the query, as it has the closest cache focus and thus most likely keeps the requested data in its cache. In case of cache misses, the node fetches missing data from the data back-end. On an arbitrary graph greedy routing does not always find the global optimum, but prematurely terminates at a local optimum which is not closest to the query region. However, it is proven in (Bose et al., 1999) that greedy routing always succeeds to find the closest node for Delaunay-based link topologies.

For performance reasons, we do not force the whole link topology to be coherent to the Delaunay property all the time, but occasionally allow minor deviations from that property in certain parts of the link structure. Consequently, the accuracy of greedy routing will degrade, as the global optimum can not always be found in a non-perfect Delaunay triangulation. Nevertheless, this does not influence the correctness of the query results as every node is able to request missing data from the data back-end. Yet, inaccurate routing may decrease the cache hit-rate, as a mislead query will be processed by a node whose cache focus is not closest to the query region and thus may not have cached as much of the requested data as the optimal node. In our system, the movement of cache foci may violate the Delaunay property in certain regions and thus decrease the cache hit-rate. Therefore it is necessary to reorganize the link structure once the routing accuracy has been decreased too much.

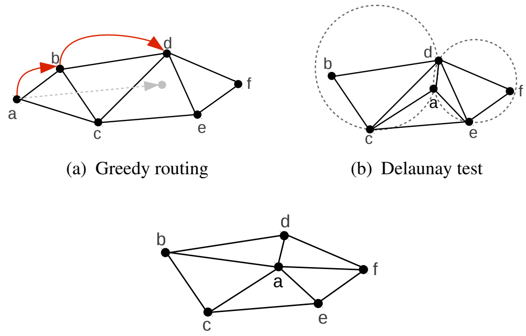

(a) Greedy routing (b) Delaunay test (c) Link reorganization

Figure 4: Move a node's cache focus position.

Network Maintenance. Particularly for application fields that can cope with partial routing inaccuracy, a set of protocols were devised which are able to establish and maintain a Delaunay-based link topology in a distributed setting under node churn, so that nodes can join or leave unexpectedly (Lee et al., 2008). Moreover, it has been shown that the topology converges to an accurate Delaunay topology once the churning has stopped. In particular, this property is extremely useful for our purposes, as it ensures that the system's efficiency returns to normal after adapting to node churn or repositioned cache foci. Thus, this maintenance protocol can be used for node joins and departures. However, to provide the flexibility needed for our multi-level load-balancing, we extend this protocol in the following section.

Network Reorganisation. The maintenance protocol outlined in the previous section can be extended by a new primitive `MOVE` which moves a node's cache focus to a certain position and updates the link structure if required. Figure 4(a) depicts an exemplary network before a node has moved. Suppose that the cache focus of node a ought to be moved into the center of triangle (c,d,e). With greedy routing (visualized as red arrows) we are able to find the closest node to the destination position which is node d in our example. Node d splits the destination triangle into three new triangles and checks whether the new triangles violate the Delaunay property. In our example it discovers that the triangles (c,a,d) and (a,e,d) violate the Delaunay property as b and f are contained by the circumcircle as shown in Figure 4(b). Then node d flips the edges (c,d) and (d,e) to obtain a triangulation as depicted in Figure 4(c). As the flipped edges may in turn violate the Delaunay property of different triangles this process is recursively repeated until no violations are found anymore. Then node d informs the involved nodes (i.e., nodes b, c, e and f) about the changed link structure. As the flipped edges may in turn violate the Delaunay property of different triangles this process is recursively repeated until no violations are found anymore.

3.3 Multi-level Load-balancing

Our multi-level load-balancing approach operates in two stages. The first stage determines a node's initial cache focus when joining the cache network. The second stage organizes the continuous repositioning of cache foci during run-time.

Initial Cache Focus Positions. When a node joins the cache network, we use an anticipated distribution, such as our examples ρ_g or ρ_c of Figure 2 to calculate the initial position. Greedy routing finds the closest node which inserts the new node into the encircling triangle of the calculated position. We assume that each node determines its initial cache focus position individually. Thereby it is crucial that all nodes use the same anticipated distribution to determine their initial position. In this manner, the nodes can autonomously organise the positions of their cache foci during the network construction and thus prepare the system layout for anticipated load patterns.

Cache Focus Update. The general idea is that nodes use ρ_h of Figure 2 to periodically calculate a new position and move their cache focus towards it. To avoid rapid zig-zag movements of cache foci and to obtain a smooth distribution of resources, we base upon standard k-means (Macqueen, 1967), which we extended to our distributed environment. Subsequently, we sketch the procedure in pseudo code:

procedure UPDATEPOSITION($P = \{p_1, p_2, \dots p_k\}$)
    Initialize indices $i_j \leftarrow 1, \forall j = 1,2\dots k$
    repeat
        $r \leftarrow$ Random point according to ρ_h
        Find the closest point $p_j \in P$ to r
        $p_j \leftarrow \frac{i_j * p_j + r}{i_j + 1}$
        $i_j \leftarrow i_j + 1$
    until Average distance of the last λ movements is lower than threshold τ
    Initiate topology re-organisation for all changed p_j.
end procedure

Each node periodically executes *UpdatePosition*, where P comprises the position of its cache focus and all the cache foci of its direct neighbors. In the interpretation of k-means, these positions resemble the centers of k clusters. In each iteration, the algorithm generates a random point r according to ρ_h, finds the closest cluster and updates the cluster center p_j. The iteration stops when the average distance of the last λ movements is lower than a threshold τ. In other words, the algorithm converges when our accuracy criterion defined by λ and τ is met. This is the state in which the points are smoothly distributed according to ρ_h. If the position of a node's cache focus has changed during the computation, it initiates a topology re-organization using the `MOVE` primitive (see Section 3.2). Empirical analysis exposed that the algorithm produces sufficient results for the values $\lambda = 20$ and $\tau = 50m$ which we used throughout all our experiments. In addition, we obtained acceptable adaption rates using an update period of 5 s.

4 EVALUATION

In this section, we focus on examining the system properties in respect to adequate resource allocation. To measure the quality of resource allocation, we begin with characterizing the adequateness of our caching strategy in respect to given data requests. To measure this aspect, we use the cache hit-rate. For a given query, we define the hit-rate as the number of objects retrieved from the cache divided by the number of objects satisfying the query. If no object satisfies the query, nodes can often avoid sending a request to the data back-end, as they internally mark empty regions. Thus, to avoid undefined values in the empty result case, we define the cache hit-rate as 1 if no back-end request was sent and 0 otherwise.

Furthermore, we look into the distribution of workload among the nodes. Thereupon, we measure the deviation of all nodes from the average workload in the system. Let avg_t be the average workload of all n nodes at a time t and ω_{tj} the workload of node j at time t, then the average deviation can be defined as:

$$\overline{dev}(t) = \frac{\sum_{j=1}^{n} |\omega_{tj} - avg_t|}{n} \tag{1}$$

From that we obtain

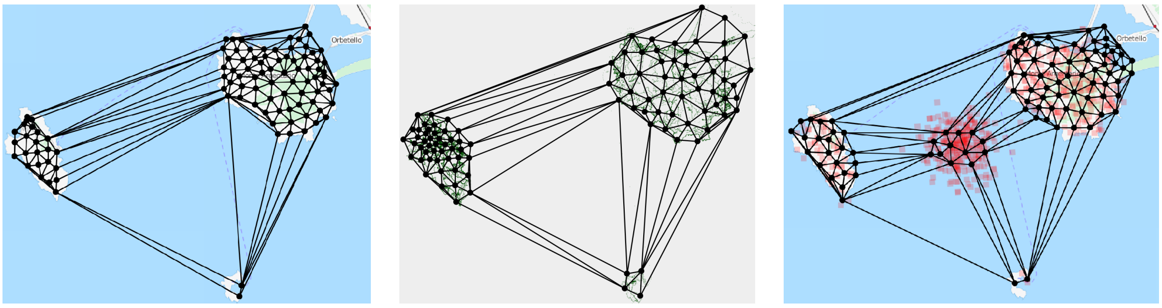

(a) Resource initialization with ρ_g (b) Resource initialization with ρ_c (c) Hot spot adaptation using ρ_h

Figure 5: Visualization of the cache network.

$$dev(t) = \frac{1}{1+\overline{dev}(t)} \tag{2}$$

which constitutes our normalized optimality measure for workload distribution.

We evaluated our approach by simulation using PeerSim (Montresor et al., 2009), which bases on a discrete event-driven simulation model. PeerSim is able to simulate peer-to-peer networks. We extended PeerSim in order to simulate our density-based spatial cache network. The simulation bases on real world data of the Italian island Giglio and its surroundings extracted from OpenStreetMap. The data set comprises a total number of 36 777 objects. It covers an area of roughly 32×35 km, in which data is not spread evenly, but rather resembles the density of geographic features in the land parts of the coastal region. On top of this data, we emulate range queries (500 x 500 m) at a rate of approximately 83 queries per second. I.e. every 12 ms a query is sent to a randomly chosen node in the cache network. The cache network comprises a total number of 100 nodes which are initialized with empty caches.

To compare our multi-level load-balancing algorithm with a purely dynamic approach, we used the load-balancing mechanism of our previous work (Lübbe et al., 2012) which bases upon a particle-spring model. In this model, the particles represent the cache foci which are interconnected by springs. Load-balancing is achieved by spring contraction in regions with high load. Furthermore, we initialized the particle-spring system by distributing the cache foci uniformly across the space in rows of 10 cache foci in each dimension. The optimization goal of the load-balancing algorithm can be tuned towards workload and cache occupancy. Workload is defined as queries per second, while cache occupancy is defined as the number objects cached by a single node divided by the area it covers. For spatial data sets that do not contain vast empty areas this is a good approximation of the data density. However, in our scenario which contains huge empty regions, this measure is imprecise which leads to faulty load-balancing. For that reason, we used a workload-only setting for all our experiments. Through a specific parameter, β, the stiffness of the particle-spring system and thus influences the adaption speed of the load-balancing algorithm can be influenced. For each of the following experiments, we empirically determined the most advantageous setting for β and compared the best results of this parameter setting with the results of our multi-level approach. In the following, we first examine the system behavior when the actual load matches anticipated workload patterns. Then we study the effects of deviation from the anticipated workload patterns.

4.1 Anticipated Workload

To examine the system behavior under anticipated workload, we initialized our system with a node capacity of 800 objects per node and distributed the cache foci according to ρ_g, i.e. a uniform distribution within land parts as visualized in Figure 5(a), and ρ_c, i.e. a data density-based distribution as depicted in Figure 5(b). Then we emulated a uniform distribution of 5 000 queries within the land parts. The simulation lasts for 1 min of simulation time. Figure 6(a) depicts the hit-rate during the simulation. One can observe a slightly better hit-rate for the data density-based distribution ρ_c. The reason for this is the concentration of cache memory in regions with a lot of data which is a more suitable resource allocation strategy for our data set. As it can be observed in Figure 5(b) data is not distributed evenly within land parts, but is slightly denser on the western island. Obviously, the more non-uniformly the data is spread within land parts, the better the data density-based resource allocation will get. Moreover, we examined the optimality of workload distribution in Figure 6(b). The geometry-based resource allocation slightly outperforms the density-based allocation, as it distributes the resources uniformly within the land parts which match exactly our expected workload. Alongside, we examined

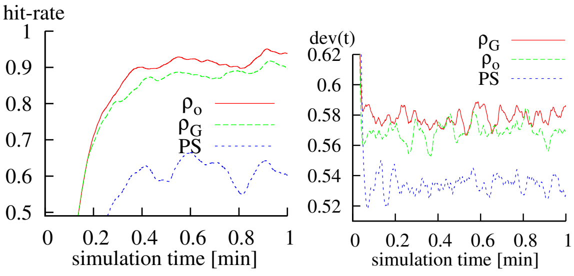

(a) width=3.5cm (b) Workload distribution

Figure 6: System parameters under anticipated workload [capacity=800].

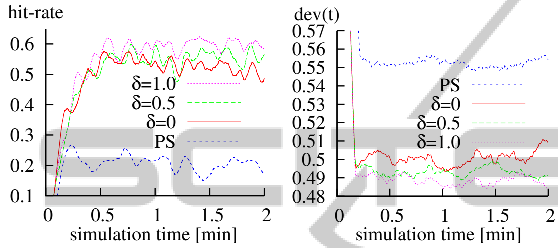

(a) Hit-rate (b) Workload distribution

Figure 7: System parameters under deviated workload [capacity=300].

our purely dynamic particle-spring approach (PS) of previous work (Lübbe et al., 2012) under the given workload using $\beta = 13$. The results show the clear supremacy of static load-balancing provided that the actual workload meets the anticipated patterns.

4.2 Deviated Workload

To examine the system performance when the actual workload deviates from anticipated patterns, we emulated a hot spot of 5 000 queries in the sea area according to a Gaussian distribution with a standard deviation of 1 500 m. The hot spot workload comes on top of anticipated workload, thus adding up to total workload of 10 000 queries. Moreover, we inspect the impact of scarce resources on the system performance. For that reason, we reduced the node capacity to 300 objects per node, i.e. with a total number of 100 nodes, the overall capacity of the cache memory sums up to 30 000 objects which is approximately 80 % of the complete data set size. We initialized our system with ρ_g (uniform distribution within land parts) and used ρ_h continuous adaptation towards the actual load. In our example ρ_h incorporates both ρ_g and ρ_d. The parameter δ allows weighting between these two aspects. Figure 7(a) depicts the hit-rate during the simulation. The most obvious result is that compared to Figure 6(a) all hit-rates have decreased. This is due to the reduced node capacity. However, the best hit rate is achieved by $\delta = 1$, i.e. when the system favors anticipated workload during load-balancing. This is because most of the cache memory is preserved for land parts where it is needed most. The hit-rate degrades slightly for lower values of δ. Contrary results can be observed for the optimality of workload distribution in Figure 7(b) where low values of δ lead to better results. In this case more nodes are assigned to process the workload of the sea area which leads to a better overall distribution of the workload between the nodes. The particle-spring approach ($\beta = 4$) performs quite well in terms of optimality of workload distribution, as it is solely focused on distributing the workload evenly among the nodes, but completely ignores other aspects. The consequence is a disastrous hit rate provoked by inadequate memory allocation.

5 CONCLUSIONS

The key aspects of load-balancing – *data skew*, *anticipated workload* and *dynamic load peaks* – can be consolidated into a single abstract mathematical model. Static load-balancing techniques can only handle the first two aspects, but are useless in the face of unpredictable load peaks. Dynamic approaches solely focus on the last issue and suffer from inadequate resource allocation.

In this paper, we take advantage of an abstract load-balancing model to implement a distributed and elastic cache infrastructure which supports multi-level load-balancing. Through multi-level load-balancing, the advantages of both static and dynamic approaches can be exploited to achieve superior load-balancing facilities. We examined our approach in a scenario of skewed data, anticipated and unpredictable workload. Compared with the purely dynamic approach of previous work (Lübbe et al., 2012), we achieved significantly better resource utilization. In our concrete scenario, we could save up to 40 % of back-end accesses in comparison to the dynamic approach.

We conducted our work with focus on the application field of spatial data processing. Beyond that, our approach can be generalized to other application fields which require high scale processing of data requests over ranges, e.g., eScience applications in the field of astrophysics. In principle, the only requirement is that the data can be numerically ordered and a distance metric exists. Thus, it is even possible to consider high-dimensional data with more than two dimensions. For future work we plan to explore different application fields and to analyse the impact of high dimensionality on our mechanism.

REFERENCES

Aberer, K. et al. (2005). Indexing data-oriented overlay networks. In *VLDB*, pages 685–696. VLDB Endowment.

Bose, P. et al. (1999). Online routing in triangulations. In *ISAAC*, pages 113–122, London, UK. Springer-Verlag.

de Berg, M. et al. (2000). *Computational Geometry: Algorithms and Applications*. Springer.

Grinstead, C. M. et al. (2006). *Grinstead and Snell's Introduction to Probability*. AMS.

Lee, D.-Y. et al. (2008). Efficient and accurate protocols for distributed delaunay triangulation under churn. In *ICNP*, pages 124–136.

Lübbe, C. et al. (2012). Elastic load-balancing in a distributed spatial cache overlay. In *MDM '12*, pages 11–20, Washington, DC, USA. IEEE.

Lübbe et al., C. (2011). DiSCO: A Distributed Semantic Cache Overlay for Location-based Services. In *MDM '11*, pages 17–26, Washington, DC, USA. IEEE.

Lübbe et al., C. (2013). Holistic Load-Balancing in a Distributed Spatial Cache. In *MDM '13*, Washington, DC, USA. IEEE.

Macqueen, J. B. (1967). Some methods of classification and analysis of multivariate observations. In *Berkeley Symp. on Mathematical Statistics and Probability*, pages 281–297.

Montresor, A. et al. (2009). PeerSim: A scalable P2P simulator. In *P2P*, pages 99–100, Seattle, USA.

Morton, G. (1966). *A Computer Oriented Geodetic Data Base and a New Technique in File Sequencing*. IBM.

Scholl, T. et al. (2009). Workload-aware data partitioning in community-driven data grids. In *EDBT*, pages 36–47, New York, USA. ACM.

Stoica, I. et al. (2001). Chord: A scalable peer-to-peer lookup service for internet appl. In *SIGCOMM*, pages 149–160, New York. ACM.

Wang, H. et al. (2005). Aspen: an adaptive spatial peer-to-peer network. In *ACM GIS*, pages 230–239, NY, USA. ACM.